CHAPTER II
LITERATURE REVIEW

2.1 Hydrogen: Fuel of the Future

Hydrogen is now being considered as an ideal fuel for the future. Hydrogen fuel can be produced from clean and renewable energy sources, and thus, its life cycle is clean and renewable. Solar and wind are the two major sources of renewable energy, and they are also the promising sources for renewable hydrogen production. However, presently, renewable energy contributes only about 5% of the commercial hydrogen production primarily via water electrolysis, while other 95% hydrogen is mainly derived from fossil fuels (Bak *et al.*, 2002). Hydrogen is a carrier of energy, not a source. It does not exist in a natural state on earth and must be reduced using a hydrogen-rich compound as the raw material. Today, hydrogen is produced mainly through steam reforming of natural gas, but it can be extracted from other hydrocarbons by reforming or partial oxidation. A major shortcoming of the processing of hydrocarbons is the resulting emissions of carbon and airborne pollutants. Most of the other production processes in use or under development involve the electrolysis of water by electricity. This method produces no emissions, but is typically more costly as compared to hydrocarbon reforming or oxidation because it requires more energy and because electricity is, in most cases, more expensive than fossil fuels. Photovoltaic water electrolysis may become more competitive as the cost continues to decrease with the technology advancement. The integration of solar energy concentration systems with systems capable of splitting water is of immense value and impact on the energetics and economics worldwide; by some is considered as the most important long-term goal in solar fuel production to cut hydrogen costs and ensure virtually zero CO_2 emissions; however, the considerable use of small band gap semiconducting materials may cause serious life cycle environmental impacts. The utilization of an oxide semiconductor photocatalyst is a promising technique because the photocatalyst is in a solid phase form and is secure for use, resistant to deactivation, chemically stable, and environmentally friendly. The diagram in Figure 2.1 shows that, while the

introduction of fuel cell technology will lead to a substantial reduction in the emissions of greenhouse gases (expressed in carbon units per kilometer), the use of fuel cells powered by hydrogen obtained from solar energy will reduce the emissions to nearly zero. Hydrogen is not present in nature in a gaseous form. However, it is abundantly available in plants, as well as in several compounds, such as methane, methanol, and higher hydrocarbons. Most importantly, it is available in water. Therefore, hydrogen must be extracted from these compounds.

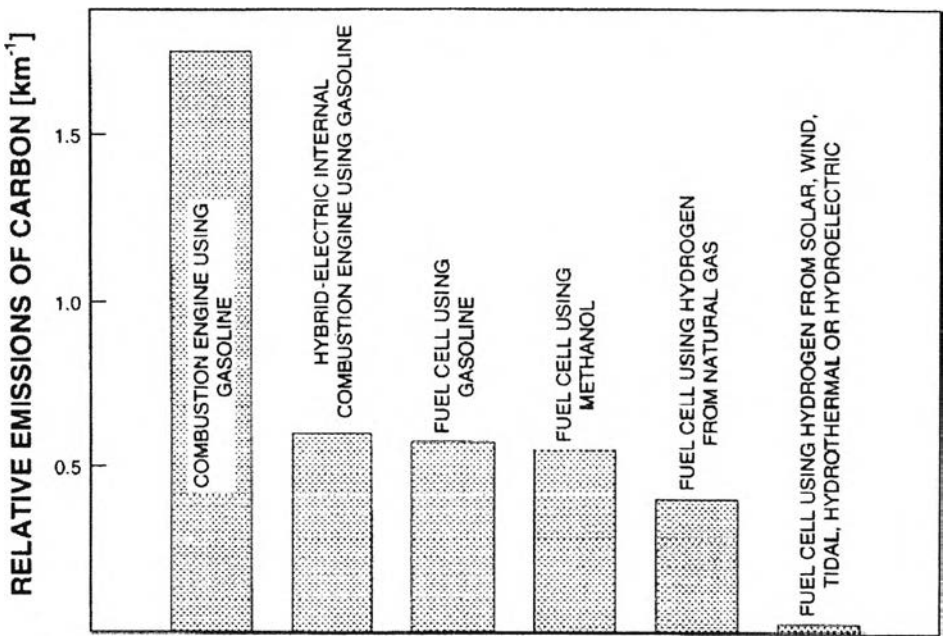

Figure 2.1 Relative emissions of greenhouse gases (expressed in carbon units per km) for vehicles powered by today's internal combustion engine using gasoline compared to vehicles powered by fuel cells (Bak *et al.*, 2002).

2.2 Water Splitting: Hydrogen Generation Using Solar Energy

The technologies for hydrogen generation from renewable energy sources of are in the incubation stage. Photocatalytic splitting water into hydrogen has attracted extensive attention due to its potential to obtain clean and highly efficient hydrogen energy from abundant water. For about 35 years, since the work of Fujishima and Honda (1972), which reported on the photodecomposition of water over semiconductor photoelectrolysis cells, many studies about the photocatalytic

splitting of water have been carried out. The energy conversion efficiency of water photoelectrolysis is primarily determined by the properties of materials used for the photoelectrodes.

For photoelectrolysis of water, a potential difference of more than 1.23 eV is necessary between cathodic and anodic electrodes (Equation (2.1)), where the following anodic and cathodic reactions take place simultaneously (Equations (2.2) and (2.3)).

$$H_2O \rightarrow H_2 + 1/2O_2, E = 1.23 \text{ eV} \quad (2.1)$$

$$2H_2O + 2e^- \rightarrow H_2 + 2OH^-, E^0 (pH = 7) = -0.41 \text{ V vs. NHE} \quad (2.2)$$

$$2H_2O \rightarrow O_2 + 4H^+ + 4e^-, E^0 (pH = 7) = +0.82 \text{ V vs. NHE} \quad (2.3)$$

This potential difference is equivalent to the energy of a wavelength of approximately 1,008 nm. Therefore, if the energy of light is used effectively in an electrochemical system, it should be possible to decompose water with visible light of wavelength shorter than 1,008 nm. However, water is transparent to visible light, so it cannot be decomposed by visible light alone. It can be split by irradiation alone only with ultraviolet light shorter than 190 nm. Fujishima and Honda (1972) were the first to study photodecomposition of water over semiconductor photoelectrolysis cells using light of wavelength $\lambda < 400$ nm. Photoelectrolysis cells consisting of a TiO_2 electrode and Pt black electrode are connected through an external load, as shown in Figure 2.2. Photo-irradiation of the TiO_2 electrode under a small electric bias leads to the evolution of H_2 and O_2 at the surface of the Pt electrode and TiO_2 electrode (Equations (2.4)-(2.6)), respectively.

$$TiO_2 + 2h\nu \rightarrow 2e^- + 2h^+ \text{ (excitation of } TiO_2 \text{ by UV light)} \quad (2.4)$$

$$2h^+ + H_2O \rightarrow 1/2O_2 + 2H^+ \text{ (at the } TiO_2 \text{ electrode)} \quad (2.5)$$

$$2e^- + 2H^+ \rightarrow H_2 \text{ (at the Pt electrode)} \quad (2.6)$$

The overall reaction can be expressed as Equation (2.7):

$$H_2O + h\nu \rightarrow 1/2O_2 + H_2 \quad (2.7)$$

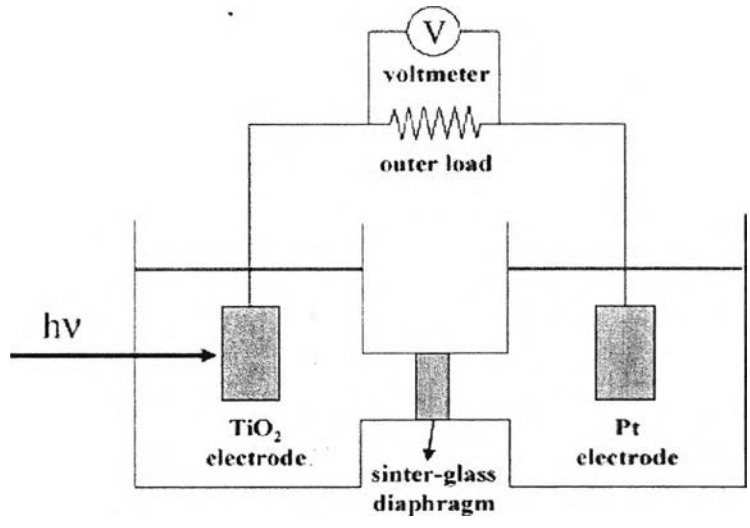

Figure 2.2 Electrochemical cell in which the TiO_2 electrode is connected with a Pt electrode (Matsuoka *et al.*, 2007).

Despite the success of Fujishima and Honda (1972), use of a photoelectrochemical cells involves the difficulty of constructing the oxide semiconductor photoelectrode. Therefore, applications of the principle of water photodecomposition using semiconductor to heterogeneous photocatalytic systems using powdered semiconductors instead of photoelectrodes have been widely studied by reason of their advantages over photoelectrochemical cells, i.e. low cost to construct, chemical stability under the light, and large surface area. Such attempts have been supported by two experimental advances. One is accumulation of data on photocatalytic reactions over powdered semiconductors, while the other is Bard's concept that can be pictured as a ''short-circuited'' photoelectrochemical cell where semiconductor electrode and metal counter electrode have been brought into contact in single particle. The history and development of the briefly mentioned progress about water splitting can be traced as follows (Bard and Fox, 1995).

2.2.1 Efficiency

The free energy change for water splitting reaction is ΔG° = 237.2 kJ/mol or 2.46 eV/molecule of H_2O. Since two electrons are involved in the reaction, this corresponds to 1.23 eV/e, which is also the standard emf for the reaction. The

photons in the solar spectrum provide sufficient energy to drive this reaction, but the efficiency of the reaction depends upon how the reaction is carried out. It is possible to cause water splitting thermally with light via concentrators and a solar furnace by heating water to 1,500-2,500 K. However, the efficiency of this process is typically below 2%, and the cost of the capital equipment and material stability problems suggest that this approach for water splitting is not a promising one.

Since water itself does not absorb appreciable ration within the solar spectrum, one or more light-absorbing species, i.e. semiconductors as the photoconverters, must be used to transform the radiant energy to chemical (or electrical) energy in the form of electron/hole pairs, i.e. to the oxidizing and reducing potentials needed to drive the reaction. The maximum efficiency for photochemical water splitting has been considered in a number of papers and depends upon the band gap (or threshold energy), E_g, of the semiconductor. Radiation of energy below E_g is not absorbed while that above E_g is partly lost as heat by internal conversion or intraband thermalization processes. Additional thermodynamic losses occur because the excited state concentration is only a fraction of that of the ground state and because some excited states are lost through radiative decay (Archer and Bolton, 1990).

2.2.2 Semiconductor

A semiconductor is a material with an electrical conductivity that is intermediate between that of an insulator and a conductor. Like other solids, semiconductor materials have electronic band structure determined by the crystal properties of the material. The actual energy distribution among electrons is described by the Fermi level and temperature of the electrons. Among the bands filled with electrons, the one with the highest potential level is referred to as the valence band (VB), while the band outside of this is referred to as the conduction band (CB). The energy width of the forbidden band between the valence band and the conduction band is referred to as the band gap (E_g). The overall structure of band gap energy is shown in Figure 2.3. The band gap can be considered as a wall that electrons must jump over in order to become free. When light is illuminated at appropriate wavelengths with energy equal or more than band gap energy, valence band (VB) electrons can move up to the conduction band (CB). At the same time, as

many positive holes as the number of electrons that have jumped to the conduction band (CB) are created.

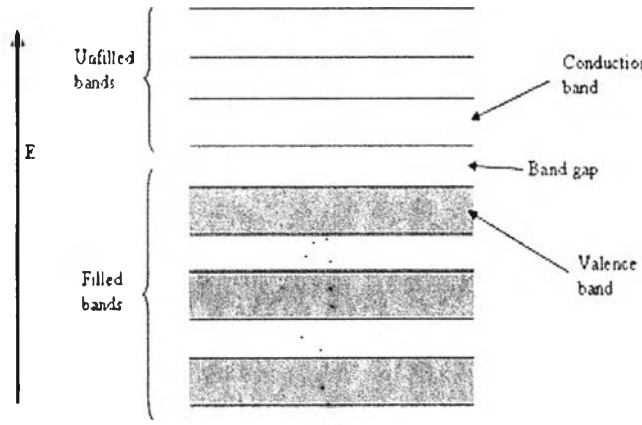

Figure 2.3 The structure of band gap energy.

2.2.3 Types of Semiconductor Systems Proposed for Solar Water Splitting

2.2.3.1 Semiconductor Solid State Photovoltaic Based Systems

A number of different approaches are possible with semiconductors. The most direct approach employs a solid state photovoltaic solar cell to generate electricity that is then passed into a commercial-type water electrolyzer, as shown in Figure 2.4(a). The electrolysis of water at a reasonable rate in a practical cell requires applied voltages significantly larger than the theoretical value (1.23 V at 25°C). Moreover, the components are rugged and should be long-lived. The problem with such a system is its cost. Solar photovoltaics cannot currently produce electricity at competitive prices, and hydrogen from water electrolyzers is significantly more expensive than that produced chemically from coal or natural gas.

An alternative system involves the semiconductor photovoltaic cell immersed directly in aqueous system, as illustrated in Figure 2.4(b). This eliminates the costs and mechanical difficulties associated with separate construction and interconnection of solar and electrochemical cells. In one such system, the electrodes are composed of single or multiple semiconductor p/n junctions that are irradiated while they are within the cell. This simpler apparatus is attained at the cost

of encapsulating and coating the semiconductors to protect them from the liquid environment and probably with a more limited choice of electrocatalyst for H_2 or O_2 evolution. Note that, in addition to p/n semiconductor junctions, those between a metal and semiconductor can also be used to produce a photopotential.

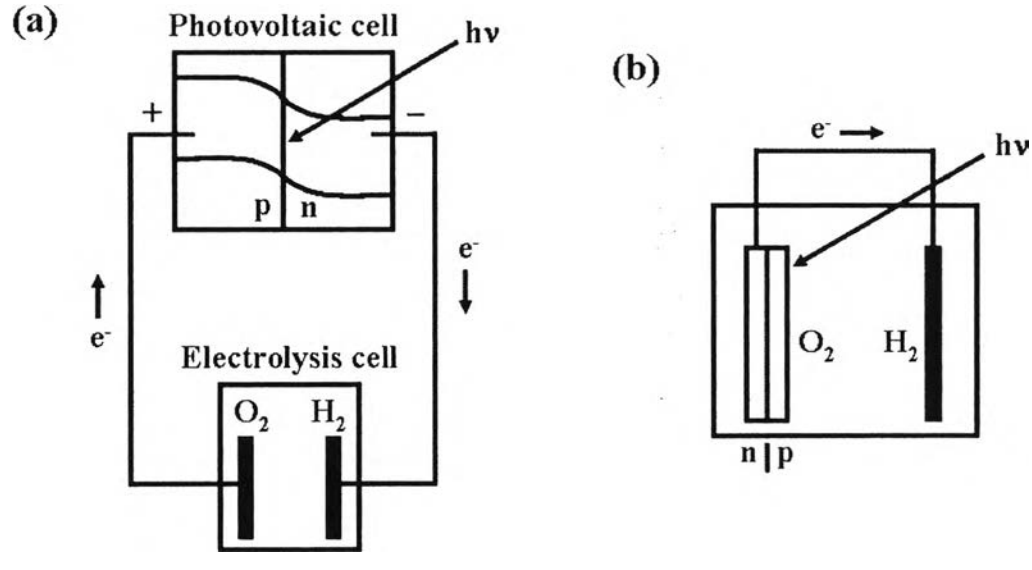

Figure 2.4 Schematic of (a) solid state photovoltaic cell driving a water electrolyzer and (b) cell with immersed semiconductor p/n junction (or metal/semiconductor Schottky junction) as one electrode.

2.2.3.2 Semiconductor Electrode (Liquid Junction) Systems

Of more interest are systems, in which the photopotential to drive the water splitting reaction is generated directly at the semiconductor/liquid interface, as shown in Figure 2.5. Rather extensive research has been carried out on various metal electrodes, sometimes covered with oxide or other films, and immersed in a variety of solutions, including some containing fluorescent dyes. The discovery of the transistor and interest in semiconductor materials led to more extensive electrochemical and photoelectrochemical studies, usually with the goal of characterizing the semiconductor.

The modern era of semiconductor electrodes and interest in these in photoelectrochemical devices for energy conversion, especially via the water splitting reaction, can be cited to the work of Fujishima and Honda (1972) on single-

crystal TiO_2 electrodes. Indeed, water splitting in TiO_2-based cells can be accomplished, but only with an additional electrical bias. The problem with TiO_2 is that the conduction band is too low, i.e. at an insufficiently negative potential, to generate hydrogen at a useful rate. Moreover, because the TiO_2 band gap is too large (3.2 eV for anatase and 3.0 eV for rutile), only a small fraction of the solar light is absorbed. Cells with TiO_2 electrodes of various types, e.g. single crystal, polycrystal, and thin film, have nevertheless been extensively investigated, mainly because TiO_2 is very stable and is a good model for understanding the semiconductor/liquid interface.

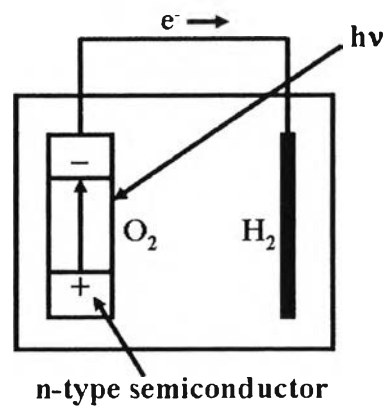

Figure 2.5 Schematic of liquid junction semiconductor electrode cell.

2.2.3.3 Semiconductor Particle Systems

A considerable simplification of the apparatus is possible if the electrochemical cell can be replaced by simple dispersions of semiconductor particles. In such dispersions, the semiconductor particles can be coated with islands of metals or metal oxides that behave as catalytic sites, with each particle behaving as a microelectrochemical cell, as shown in Figure 2.6. TiO_2 has been a favorite material, although other compounds, such as CdS and ZnO, have also been studied. While a number of interesting photoreactions have been carried out, including the use of particles to destroy organics and to plate metals from wastewater (Ollis and Al-Ekabi, 1993) and for synthetic purposes (Serpone and Pelizzetti, 1989), reports on the use of particulate systems for water splitting remain controversial. An extension

of this approach is the use of colloidal-sized particles down to nanoparticles. Such small particles also have very high surface areas that, in principle, allow faster capture of the photogenerated charges by solution species and with less bulk recombination.

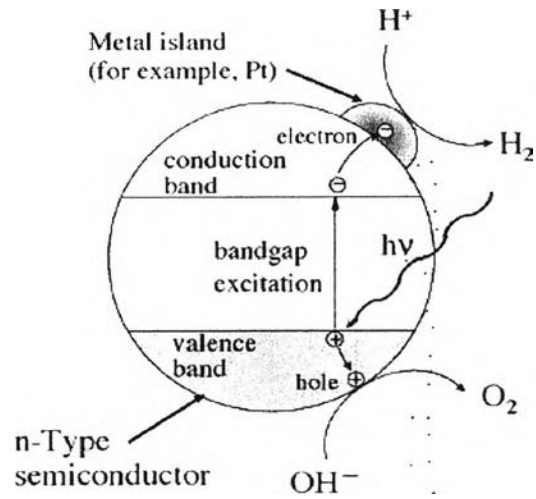

Figure 2.6 Representation of semiconductor particulate system for heterogeneous photocatalysis (Matsuoka *et al.*, 2007).

2.3 Photocatalysis and Photocatalysts for Hydrogen Generation

2.3.1 Photocatalytic Reactions

Photocatalytic reactions have been extensively studied for various applications. Photocatalytic reactions are classified into two categories: ''down-hill'' and ''up-hill'' reactions. Degradation, such as photo-oxidation of organic compounds using oxygen molecules, is generally a down-hill reaction, of which the reaction proceeds irreversibly. In this reaction, a photocatalyst works as a trigger to produce O_2^-, HO_2, OH•, and H^+ as active species for oxidation at the initial stage. This type of reaction is regarded as a photo-induced reaction, as depicted in Figure 2.7(a), and has been extensively studied using titanium dioxide photocatalyst (Fujishima *et al.*, 2000). On the other hand, water splitting reaction is accompanied by a largely positive change in the Gibbs free energy (ΔG^0 = 237 kJ/mol) and is an up-hill reaction. In this reaction, photon energy is converted into chemical energy, as also

shown in Figure 2.7(b), similar to photosynthesis by green plants. Therefore, this type of reaction is called artificial photosynthesis.

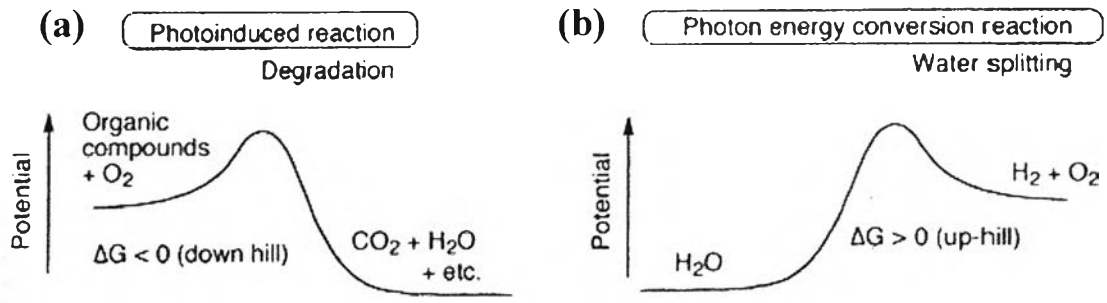

Figure 2.7 Types of photocatalytic reactions: (a) photoinduced reaction and (b) photon energy conversion reaction.

Since the first energy crisis in the early 1970s, much research has been devoted to the development of efficient systems that would enable the absorption and conversion of solar light into useful chemical energy resources. One of the most promising "artificial photosynthesis" reactions is the photocatalytic splitting of water to produce H_2 and O_2 under solar light irradiation:

$$H_2O \rightarrow H_2 + 1/2O_2,\ \Delta G^0 = 237\ \text{kJ/mol} \qquad (2.8)$$

The refinement of this up-hill reaction is greatly desired not only for the conversion and storage of solar energy but also for the clean and safe production of hydrogen since the consumption of hydrogen will be expected to increase dramatically, especially for use in fuel cells.

2.3.2 Photocatalytic Water Splitting Process

The principle of water splitting using a semiconductor photocatalyst is shown in Figure 2.8. The semiconductor photocatalyst absorbs impinging photons with energies equal to or higher than its band gap or threshold energy. Each photon of the required energy (i.e. wavelength) that strikes an electron in the occupied valence band (VB) of the semiconductor atom can elevate that electron to the unoccupied conduction band (CB), leading to excited state conduction band electrons and positive valence band holes (Serpone and Pelizzetti, 1989). The photogenerated electrons and holes cause redox reactions similar to electrolysis. Water molecules are reduced by the electrons to form H_2 and oxidized by the holes to form O_2, leading to

overall water splitting. The width of the band gap and the potentials of the conduction and valence bands are important for the semiconductor photocatalyst material. The bottom level of the conduction band (CB) has to be more negative than the reduction potential of H^+/H_2 (0 V vs NHE), while the top level of the valence band (VB) has to be more positive than the oxidation potential of O_2/H_2O (1.23 V).

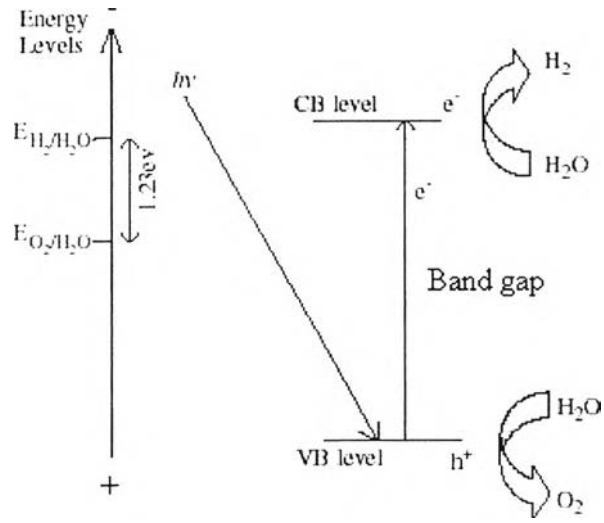

Figure 2.8 Reaction schematic for water splitting reaction over semiconductor photocatalysts.

The competition between charge carrier recombination and charge carrier trapping followed by the competition between recombination of trapped carriers and interfacial charge transfer are what determine the overall quantum efficiency for interfacial charge transfer. Also of great importance are the band positions or flat band potentials of the semiconductor material. These indicate the thermodynamic limitations for the photoreactions that can take place.

However, the potential of the band structure is just the thermodynamic requirement. Other factors, such as chare separation, mobility, and lifetime of photogenerated electrons and holes, also affect the photocatalytic properties, as shown in Figure 2.9, in which the fate of these charge carriers may take different paths. Firstly, they can get trapped in the bulk either in shallow or in deep traps.

Secondly, they can recombine, non-radiatively or radiatively, dissipating the input energy as heat. Finally, they can react with electron donors or acceptors adsorbed on the surface of the photocatalyst (Hoffmann *et al.*, 1995). These properties are strongly influenced by bulk properties of the material, such as crystallinity. Surface properties, such as surface area and active reaction sites, are also imperative. Cocatalysts, such as Pt and NiO, are often loaded on the surface in order to introduce active sites for H_2 evolution. Thus, suitable bulk and surface properties and energy structure are demanded for effective photocatalysts. So, one can state that the photocatalyst is a highly functional material.

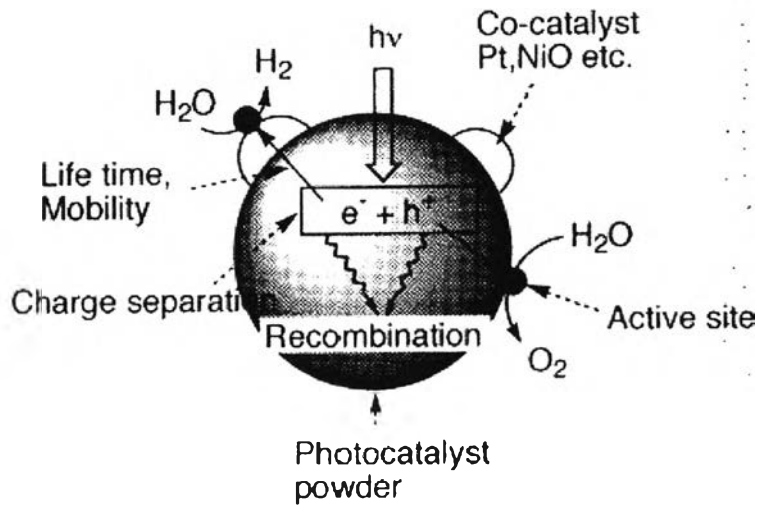

Figure 2.9 Processes occurring in semiconductor photocatalyst under photoexcitation for water splitting reaction

2.3.3 Photocatalysts

Since water is transparent to solar radiation, direct decomposition of water by solar light is not viable. Energetically, it seems relatively easy to photocatalyze water, since the theoretical minimum photovoltage required for this process is only 1.23 eV. Semiconductors, in the presence of light energy, are capable of decomposing water into hydrogen and oxygen depending upon energy levels of their conduction and valence bands. In an ideal system, conduction band level should be well above (more negative than) the water reduction level, and valence band edge should be well below (more positive than) the water oxidation level for an efficient

production of hydrogen and oxygen from water by photolysis, as shown in Figure 2.10. Some of the photocatalysts that satisfy both conditions are TiO_2, $SrTiO_3$, $CaTiO_3$, $Sr_2Nb_2O_5$, $Sr_2Ta_2O_7$, ZnO, CdS, NiO, etc. However, most of these materials could not potentially used due to either wide band gap energy or photocorrosive nature, since a semiconductor photocatalyst should ideally be chemically and biologically inert, photocatalytically stable, easy to produce and to use, efficiently activated by sunlight, able to efficiently catalyze the reaction, inexpensive, and without risks for both the environment and human beings.

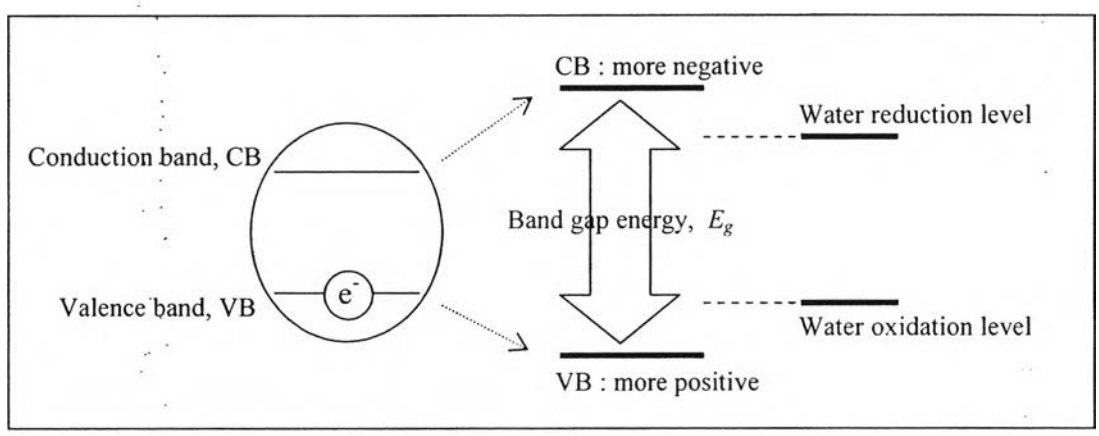

Figure 2.10 Band gap energy of the photocatalyst.

Titanium dioxide (TiO_2), the most extensively investigated semiconductor in the literature, seems to be the most promising material for photocatalytic water splitting. This semiconductor provides the best compromise between photocatalytic performance and stability in aqueous media. On the other hand, binary metal sulfide semiconductors, such as CdS and PbS, are regarded as insufficiently stable for photocatalysis, at least in aqueous media as they readily undergo photocorrosion. These materials are also known to be toxic. Fe_2O_3 is not a suitable semiconductor as it readily undergo photocorrosion, as well (Hoffmann *et al.*, 1995). Moreover, the band gap of ZnO (3.2 eV) is equal to that TiO_2; however, ZnO is also unstable in water with $Zn(OH)_2$ being formed on the particle surface. This results in a rapid photocatalyst deactivation (Howe, 1998).

2.4 Titanium Oxide Photocatalyst

2.4.1 General Remarks

TiO_2 belongs to the family of transition metal oxides. TiO_2 has received a great deal of attention due to its chemical stability, non-toxicity, low cost, and other advantageous properties. Particularly, TiO_2 is extensively utilized in solar energy conversion, i.e. solar cell and photocatalysis applications (Hoffmann *et al.*, 1995). As a result of its high refractive index, it is used as anti-reflection coating in silicon solar cells and in many thin film optical devices. TiO_2 is successfully used as gas sensor (due to the dependence of the electric conductivity on the ambient gas composition) and is utilized in the determination of oxygen and carbon monoxide concentrations at high temperatures (> 600°C), by simultaneously determining CO/O_2 and CO/CH_4 concentrations (Savage *et al.*, 2001). Due to its hemocompatibility with the human body, TiO_2 is also used as a biomaterial (as bone substituent and reinforcing mechanical supports).

2.4.2 Crystal Structure and Properties

The main four polymorphs of TiO_2 found in nature are anatase (tetragonal), brookite (orthorhombic), rutile (tetragonal), and TiO_2 (B) (monoclinic). The structures of rutile, anatase, and brookite can be discussed in terms of (TiO_2^{6-}) octahedrals. The three crystal structures differ by the distortion of each octahedral and by the assembly patterns of the octahedral chains. Anatase can be regarded to be builtup from octahedrals that are connected by their vertices; in rutile, the edges are connected; and in brookite, both vertices and edges are connected, as shown in Figure 2.11 (Carp *et al.*, 2004).

Thermodynamic calculations based on calorimetric data predict that rutile is the most stable phase at all temperatures and pressures up to 60 kBar. The small differences in the Gibbs free energy (4-20 kJ/mol) among the three phases suggest that the metastable polymorphs are almost as stable as rutile at normal pressures and temperatures. Particle size experiments affirm that the relative phase stability may reverse when particle sizes decrease to sufficiently low values due to surface energy effects (surface free energy and surface stress, which depend on particle size). If the particle sizes of the three crystalline phases are equal, anatase is

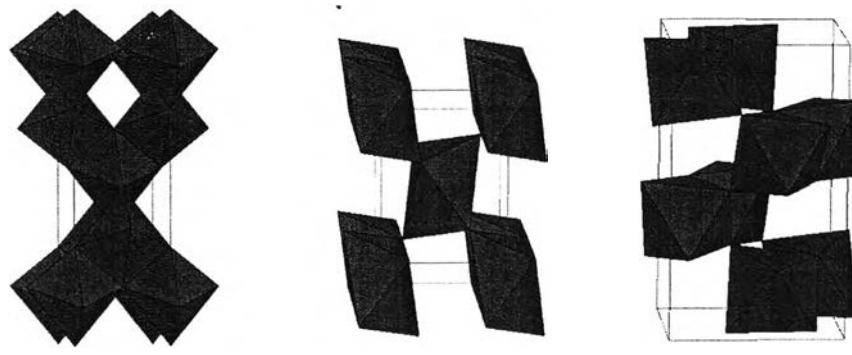

(a) (b) (c)

Figure 2.11 Crystal structures of (a) anatase, (b) rutile, and (c) brookite.

the most thermodynamically stable at sizes less than 11 nm, brookite is the most stable between 11 and 35 nm, and rutile is the most stable at sizes greater than 35 nm (Zhang *et al.*, 2000).

The enthalpy of the anatase-rutile phase transformation is low. However, there are widespread disagreement in the value, which ranges from -1.3 to -6.0 ± 0.8 kJ/mol. Kinetically, anatase is stable, i.e. its transformation into rutile at room temperature is so slow that the transformation practically does not occur. At macroscopic scale, the transformation reaches a measurable speed for bulk TiO_2 at temperature greater than 600°C. During the transformation, anatase pseudoclose-packed planes of oxygen are retained as rutile close-packed planes, and a co-operative rearrangement of titanium and oxygen ions occurs within this configuration. The proposed mechanism implies at least spatial disturbance of the oxygen ion framework and a minimum breaking of Ti–O bonds as a result of surface nucleation and growth. The nucleation process is very much affected by the interfacial contact in nanocrystalline solids, and once initiated, it quickly spreads out and grain growth occurs (Ding and Liu, 1998).

The anatase-rutile transformation has been studied for both mechanistic and application-driven reasons, because the TiO_2 phase (i.e. anatase or rutile) is one of the most critical parameters determining the use as a photocatalyst, catalyst, or as ceramic membrane material. This transformation, achieved by increased temperature

or pressure, is influenced by several factors, such as concentration of lattice and surface defects, particle size, and applied temperature and pressure.

In photocatalysis applications, both crystal structures, i.e. anatase and rutile, are commonly used, with anatase showing a greater photocatalytic activity for most reactions. It has been suggested that this increased photoreactivity is due to anatase's slightly higher Fermi level, lower capacity to adsorb oxygen, and higher degree of hydroxylation (i.e. number of hydroxyl groups on the surface). Reactions, in which both crystalline phases have the same photoreactivity (Deng *et al.*, 2002) or rutile exhibiting a higher one, (Mills *et al.*, 2003) are also reported. Furthermore, there are also studies, which claim that a mixture of anatase (70-75%) and rutile (30-25%) is more active than pure anatase (Mugglie and Ding, 2001). The disagreement of the results may lie in the intervening effect of various coexisting factors, such as specific surface area, pore size distribution, crystal size, and preparation methods, or in the way the activity is expressed. The behavior of Degussa P-25 commercial TiO_2 photocatalyst, consisting of a mixture of anatase and rutile in an approximate proportion of 80/20, is more active than both the pure crystalline phases for many reactions. The enhanced activity arises from the increased efficiency of the e^-/h^+ separation due to the multiphase nature of the particles. Water splitting reaction is a special case because band bending is necessary in order to reduce and oxidize water.

2.4.3 Semiconductor Characteristic and Photocatalytic Activity

Due to oxygen vacancies, TiO_2 is an n-type semiconductor. A semiconductor photocatalyst is characterized by its capability to adsorb simultaneously two reactants, which can be reduced and oxidized by a photonic activation through an efficient absorption ($h\nu \geq E_g$). The ability of a semiconductor to undergo photoinduced electron transfer to an adsorbed particle is governed by the band energy positions of the semiconductor and the redox potential of the adsorbates. The energy level at the bottom of conduction band is actually the reduction potential of photoelectrons. The energy level at the top of valence band determines the oxidizing ability of photogenerated holes, each value reflecting the ability of the system to promote reductions and oxidations. The flat band potential (V_{fb}) locates the energy of both charge carriers at the semiconductor-electrolyte interface, depending on the nature of the material and system equilibrium. From the thermodynamic point

of view, adsorbed couples can be reduced photocatalytically by conduction band electrons if they have more positive redox potentials than V_{fb} of the conduction band, and can be oxidized by valence band holes if they have more negative redox potentials than V_{fb} of the valence band (Rajeshwar, 1995).

Unlike metals, semiconductors lack a continuum of interband states to assist the recombination of electron-hole (e^-/h^+) pairs, which assure a sufficiently long life time of the pairs to diffuse to the photocatalyst surface and initiate a redox reduction. The differences in lattice structures of anatase and rutile TiO_2 cause different densities and electronic band structures, leading to different band gaps (for bulk materials: anatase 3.20 eV and rutile 3.02 eV). Therefore, the absorption thresholds correspond to wavelengths of 384 and 410 nm for the two TiO_2 forms, respectively. The mentioned values concern single crystals or well-crystallized samples. Higher values are usually obtained for weakly crystallized thin films or nanosized materials. The blue shift of the fundamental absorption edge in TiO_2 nanosized materials has been observed amounting to 0.2 eV for crystallite sizes in the range of 5-10 nm.

As mentioned, TiO_2 has been most widely used for studies of photocatalytic water splitting, because of its high stability against photocorrosion and its favorable band-gap energy. Presently, the energy conversion efficiency from solar to hydrogen by TiO_2 photocatalytic water-splitting is still low, mainly due to the following reasons:

- Recombination of photo-generated electron/hole pairs: CB electrons can recombine with VB holes very quickly and release energy in the form of unproductive heat or photons;
- Fast backward reaction: Decomposition of water into hydrogen and oxygen is an energy increasing process, thus backward reaction (recombination of hydrogen and oxygen into water) easily proceeds;
- Inability to utilize visible light: The band gap of TiO_2 is about 3.2 eV, and only UV light can be utilized for hydrogen production. Since the UV light only accounts for about 4% of the solar radiation energy while the visible light contributes about 50%, the inability to utilize visible light limits the efficiency of solar photocatalytic hydrogen production.

In order to resolve the above mentioned problems and make solar photocatalytic hydrogen production feasible, continuous efforts have been made to promote the photocatalytic activity and enhance the visible light response. Addition of electron donors (hole scavengers), addition of carbonate salts, noble metal loading, metal ion doping, anion doping, dye sensitization, composite semiconductors, metal ion-implantation, etc., were investigated, and some of them have been proved to be useful to enhance hydrogen production. The above listed techniques influencing H_2 production have been grouped under two broad classifications as 'chemical addition' and 'photocatalyst modification' techniques, as described later.

2.5 Nano-Photocatalysts

2.5.1 General Remarks

Nanocrystalline photocatalysts are ultra-mall semiconductor particles, which are few nanometers in size. During the past decade, the photochemistry of nanosized semiconductor particles has been one of the fastest growing research areas in physical chemistry. The interest in these small semiconductor particles originates from their unique photophysical and photocatalytic properties. Several review articles have been published concerning the photophysical properties of nanocrystalline semiconductors. Such studies have demonstrated that some properties of nanocrystalline semiconductor particles are in fact different from those of bulk materials.

Nanosized particles possess properties falling into the region of transition between the molecular and bulk phases. In the bulk material, the electron excited by light absorption funds a high density of states in the conduction band, where it can exist with different kinetics energies. In the case of nanoparticles, however, the particle size is the same as or smaller than the size of the first excited state. Thus, the electrons and holes generated upon illumination cannot suit into such a particle, unless they assume a state of higher kinetics energy. Hence, as the size of the semiconductor particle is reduced below a critical diameter, the spatial confinement of the charge carriers within a potential well, like ''a particle in a box'', causes them to mechanically behave quantum. In solid state terminology, this means

that the bands split into discrete electronic states (quantized levels) in the valence and conduction bands, and the nanoparticle progressively behaves similar to a giant atom. Nanosized semiconductor particles, which exhibit size-dependent optical and electronic properties, are called quantized particles or quantum dots (Kamat, 1995).

2.5.2 Activity of Nano-Photocatalysts

One of the main advantages of the application of nanosized particles is the increase in the band gap energy with decreasing particle size. As the size of a semiconductor particle falls below the critical radius, the charge carriers begin to behave mechanically quantum, and the charge confinement leads to a series of discrete electronic states. As a result, there is an increase in the effective band gap and a shift of the band edges. Thus by varying the size of the semiconductor particles, it is possible to enhance the redox potential of the valence band holes and the conduction band electrons.

However, the solvent reorganizational free energy for charge transfer to a substrate remains unchanged. The increasing driving force and the unchanged solvent reorganizational free energy are expected to lead to an increase in the rate constants for charge transfer at the surface. The use of nanosized semiconductor particles may result in an increased photocatalytic activity for systems, in which the rate-limiting step is interfacial charge transfer. Hence, nanosized semiconductor particles can possess enhanced photoredox chemistry with reduction reactions, which might not otherwise proceed in bulk materials, being able to occur readily using sufficiently small particles. Another factor, which could be advantageous, is the fact that the fraction of atoms that are located at the surface of a nanoparticle is very large. Nanosized particles also have high surface area-to-volume ratios, which further enhances their catalytic activity. One disadvantage of nanosized particles is the need for light with a shorter wavelength for photocatalyst activation. Thus, a smaller percentage of a polychromatic light source will be useful for photocatalysis.

In large TiO_2 particles (Zhang *et al.*, 1998), volume recombination of the charge carriers is the dominant process and can be reduced by a decrease in particle size. This decrease also leads to an increase in the surface area, which can be translated as an increase in the available surface active sites. Thus, a decrease in particle size should also result in higher photonic efficiencies due to an increase in

the interfacial charge carrier transfer rates. However, as the particle size is lowered below a certain limit, surface recombination processes become dominant, since firstly most of the electrons and holes are generated close to the surface, and secondly surface recombination is faster than interfacial charge carrier transfer processes. This is the reason why there exists an optimum particle size for maximum photocatalytic efficiency.

2.6 Chemical Additive for Enhancement of Photocatalytic H_2 Production

Due to rapid recombination of photogenerated CB electrons and VB holes, it is difficult to achieve water splitting for hydrogen production using TiO_2 photocatalyst in pure distilled water. Adding electron donors (sacrificial reagents or hole scavengers) to react irreversibly with the photogenerated VB holes can enhance the electron/hole separation, resulting in higher quantum efficiency. Since electron donors are consumed in photocatalytic reaction, continual addition of electron donors is required to sustain hydrogen production.

Organic hydrocarbon-based compounds are widely used as electron donors for photocatalytic hydrogen production as they can be oxidized by VB holes. The remaining strong reducing CB electrons can reduce protons to hydrogen molecules. EDTA, methanol, ethanol, CN^-, lactic acid, and formaldehyde have been tested and proved to be effective to enhance hydrogen production. Nada *et al.* (2005) carried out a qualitative investigation to study the effects of different electron donors on hydrogen production. The rankings in terms of the degree of hydrogen production enhancement capability were found to be: EDTA > methanol > ethanol > lactic acid. It should be noted that the decomposition of these hydrocarbons could also contribute to a higher hydrogen yield since hydrogen is one of their decomposed products. Other inorganic ions, such as S^{2-}/SO_3^{2-}, Ce^{4+}/Ce^{3+}, and IO_3^-/I^- were also used as sacrificial reagents for hydrogen production. When CdS is used as photocatalyst for hydrogen production from water splitting, photocorrosion occurs as follows:

$$CdS + 2h^+ \rightarrow Cd^{2+} + S \qquad (2.9)$$

By serving as a sacrificial reagent, S^{2-} can react with 2 holes to form S. The aqueous SO_3^{2-} added can dissolve S into $S_2O_3^{2-}$ in order to prevent any detrimental deposition of S onto CdS. Therefore, photocorrosion of CdS is prevented. In another system of using inorganic ions, I^- (electron donor) and IO_3^- (electron acceptor) work as a pair of redox mediators. Two photocatalysts can be employed to produce H_2 and O_2 under the mediation of I^- and IO_3^-, respectively. For hydrogen production on the photocatalyst with more negative CB level, I^- can scavenge holes and, thus, CB electrons are available to reduce protons to hydrogen molecules. For oxygen production on the photocatalyst with more positive VB level, IO_3^- can react with CB electrons to form I^- and, thus, VB holes can oxidize water to oxygen. In this system, photocatalytic water splitting produces both hydrogen and oxygen without consumption of the sacrificial reagent, as illustrated in Figure 2.12. As rutile TiO_2 has unique selectivity in oxidation, oxygen molecules are evolved. For comparison, IO_3^- anions are produced on the surface of anatase TiO_2. Therefore, the combination of anatase and rutile TiO_2 shows a higher hydrogen production rate under the mediation of I^-/IO_3^- pairs. Similarly, Ce^{4+}/Ce^{3+} and Fe^{3+}/Fe^{2+} pairs are also effective for hydrogen production from water splitting.

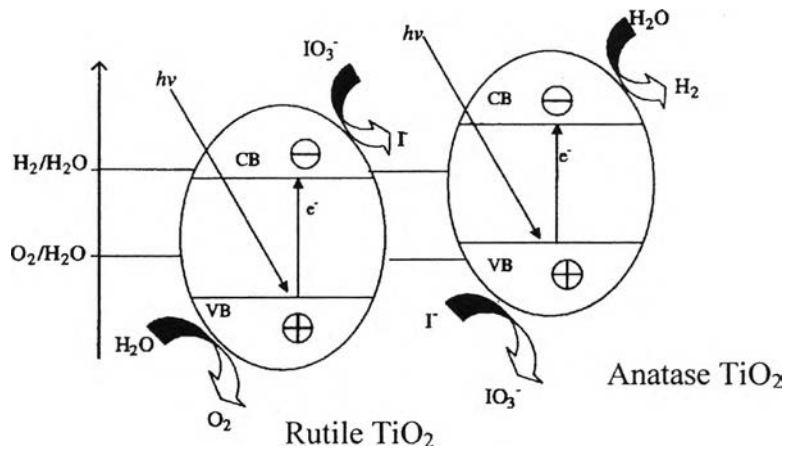

Figure 2.12 Photocatalytic hydrogen production over anatase/rutile TiO_2 under the mediation of I^-/IO_3^-.

2.7 Dye Sensitization

Dye sensitization is widely used to utilize visible light for energy conversion. Some dyes having redox property and visible light sensitivity can be used in solar cells, as well as photocatalytic systems (Gurunathan *et al.*, 1997). Under illumination by visible light, the excited dyes can inject electrons to CB of semiconductors to initiate the catalytic reactions, as illustrated in Figure 2.13. Even without semiconductors, some dyes, for example safranine O/EDTA and T/EDTA, are able to absorb visible light and produce electrons as reducing agents strong enough to produce hydrogen (Bi and Tien, 1984). Nevertheless, without semiconductors acting as efficient charge seperators, the rate of hydrogen production only by dyes is very low.

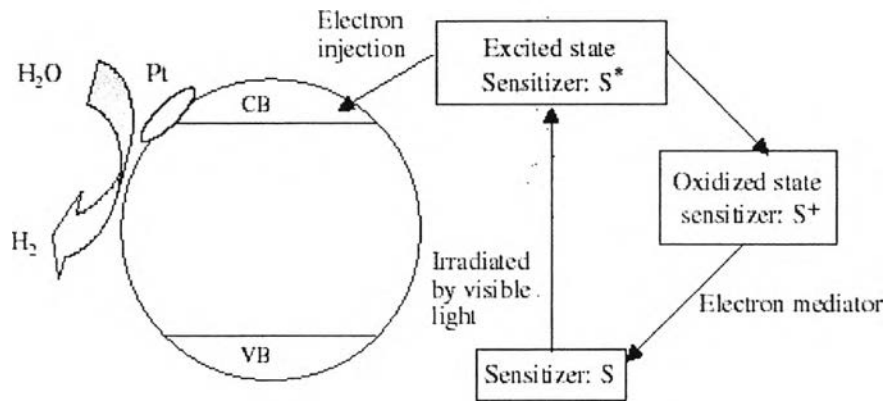

Figure 2.13 Mechanism of dye-sensitized photocatalytic hydrogen production under visible light irradiation.

High hydrogen production rate can be obtained by efficient absorption of visible light and efficient transfer of electrons from excited dyes to CB of TiO_2. The CB electrons can then be transferred to noble metal particle (such as Pt) loaded on surface to initiate water reduction. In order to regenerate dyes, redox systems or sacrificial agents, such as I_3^-/I^- pair and EDTA, can be added to the solution to sustain the reaction cycle. The excitation, electron injection, and dye regeneration can be expressed as follows:

$$dye + hv \rightarrow dye^* \quad (2.10)$$

$$dye^* + TiO_2 \rightarrow dye^+ + \cdot e^- \quad (2.11)$$

$$dye^+ + e^- \rightarrow dye \quad (2.12)$$

To obtain a higher efficiency in converting absorbed light into direct electrical energy (for solar cells) or hydrogen energy, fast electron injection and slow backward reaction are required. Based on the literature on electron/hole recombination of dyes, the recombination times have been found to be mostly in the order of nanoseconds to microseconds, sometimes in milliseconds, while the electron injection times were in the order of femtoseconds. The fast electron injection and slow backward reaction make dye-sensitized semiconductors feasible for energy conversion.

Gurunathan *et al.* (1997) investigated the effects of different dyes on photocatalytic hydrogen production by SnO_2 with and without a sacrificial agent, such as EDTA. The band gap of SnO_2 is 3.5 eV and, hence, it could not be excited by visible light. After SnO_2 was sensitized by dyes, hydrogen production was observed under visible light illumination. Qualitatively, the ranking of dyes in terms of the degree of enhancement of hydrogen production rate was found in the following order: Eosin Blue > Rose Bengal > $Ru(bpy)_3^{2+}$ > Rhodamine B ~ Acriflavin > Fluorescein. However, based on the structures and properties of these dyes, a general conclusion could not be clearly drawn. For example, Rhodamine B showed the longest absorption wavelength maxima together with more negative reduction potential (-0.545 V) than CB level (-0.34 V) of SnO_2, but it did not increase hydrogen production rate significantly. Therefore, the difference in their electron injection characteristics may be the reason for the variation in hydrogen production rates. However, comparison of electron injection characteristics among these dyes was not available. Further research work is thus required to compare dynamics of charge excitation, recombination, and electron injection of different dyes to gain a better understanding of the mechanisms behind the phenomena.

2.8 Composite Semiconductors

Semiconductor composite (coupling) is another method to utilize visible light for hydrogen production. When a large band gap semiconductor is coupled with a small band gap semiconductor with a more negative CB level, CB electrons can be injected from the small band gap semiconductor to the large band gap semiconductor. Thus, a wide electron-hole separation is achieved, as shown in Figure 2.14. The process is similar to dye sensitization. The difference is that electrons are injected from one semiconductor to another semiconductor, rather than from excited dye to semiconductor. Successful coupling of the two semiconductors for photocatalytic water splitting hydrogen production under visible light irradiation can be achieved when the following conditions are met: (1) semiconductors should be photocorrosion-free, (2) the small band gap semiconductor should be able to be excited by visible light, (3) the CB of the small band gap semiconductor should be more negative than that of the large band gap semiconductor, (4) the CB of the large band gap semiconductor should be more negative than the reduction potential of H^+/H_2, and (5) electron injection should be fast, as well as efficient.

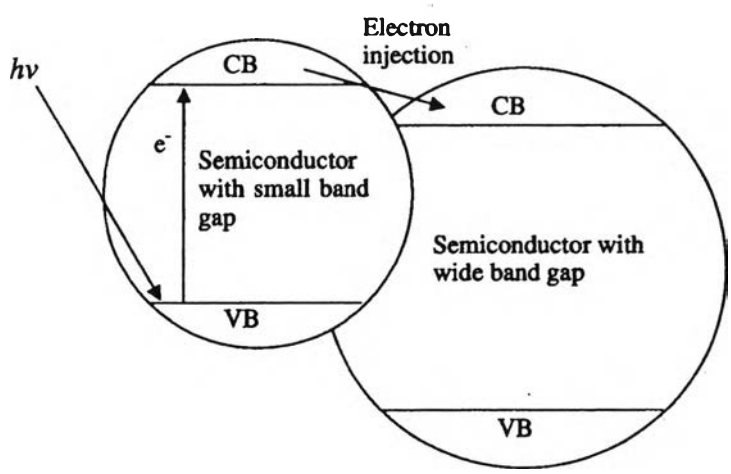

Figure 2.14 Electron injection in composite semiconductors.

It has been reported that coupling of CdS (band gap of 2.4 eV) with SnO_2 (band gap of 3.5 eV) could produce hydrogen under visible radiation (Gurunathan *et al.*, 1997). Electron excited to the CB (-0.76 eV) of CdS are injected to the CB (-0.34 eV) of SnO_2 in less than 20 ps, resulting in wide electron-hole separation. Sacrificial

agent, EDTA, has to be added to scavenge VB hole on CdS; otherwise, photocorrosion of CdS would occur. Doong *et al.* (2001) coupled CdS with TiO_2 for 2-chlorophenol degradation under UV irradiation. In the study, both CdS and TiO_2 could be excited. The combination of the two semiconductors showed better photocatalytic activity due to better charge separation. The CB electrons of CdS are injected to the CB of TiO_2, while the VB holes in TiO_2 are injected to the VB of CdS. Kang *et al.* (1999) employed CdS-TiO_2 composite semiconductor for 4-chlorophenol photodegradation and found that coupling of CdS with TiO_2 was more effective than CdS and TiO_2 used separately. The composite semiconductor of CdS-TiO_2 can be applied to produce hydrogen since the CB of TiO_2 is more negative than hydrogen production level. So *et al.* (2004) conducted photocatalytic hydrogen production using CdS-TiO_2 composite semiconductors. Photocorrosion of CdS was prevented by addition of Na_2S. Optical absorption spectra analysis showed that CdS-TiO_2 could absorb photons with wavelength up to 520 nm. Under visible light illumination (Xe lamp), CdS-TiO_2 composite semiconductors produced hydrogen at a higher rate than CdS and TiO_2 used separately.

Recently, Li *et al.* (2004) developed a novel photocatalyst by coupling nitrogen doping and composite semiconductors. Nitrogen-doped ZnO was coupled with WO_3, V_2O_5, and Fe_2O_3 for acetaldehyde decomposition under visible light irradiation. By doping with nitrogen, ZnO could respond with visible spectrum. Unlike coupling with WO_3 and V_2O_5, coupling with Fe_2O_3 causes the photocatalytic activity to deteriorate since Fe_2O_3 served as both an electron sink and a hole sink. Although N-doped ZnO-WO_3 and ZnO-V_2O_5 worked better under visible light irradiation for acetaldehyde decomposition, they were not suitable for hydrogen production since the CB of both WO_3 and V_2O_5 are not negative enough. It is expected that a N-doped composite semiconductor with CB level more negative than hydrogen production level, such as SiC-TiO_2, may serve as an efficient photocatalyst for hydrogen production under visible light irradiation.

2.9 Mixed Oxide System

The investigation of a mixed oxide system is very promising issue since such a system can be used as a base for new composite materials. The characteristics of such materials can be regulated and controlled in advance through changes in their composition. Investigations have proved good prospects for designing materials containing a photoactive semiconductor (TiO_2) and an admixture of a semiconductor (ZnO, Al_2O_3, Bi_2O_3, ZrO_2, HfO_2, V_2O_5, WO_3, etc.) with different chemical compositions. The latter substances are also widely used as pigments and catalysts, components of photolayers, and dielectric materials. They can also be used as promising source materials for ceramics. The same materials can be used for solar energy transformation and accumulation, toxic industrial waste treatment, in information recording systems, and in new industrial lines of low-tonnage synthesis of important products (Kobasa and Kondratyeva, 2008).

Incorporation of heteroatoms occurs at either cationic or anionic sites of the TiO_2 lattice, along with the formation of junctions with a second semiconductor. An interesting example of this approach is the synthesis of TiO_2-ZrO_2 photocatalysts with different compositions and phase distributions (Hernández-Alons *et al.*, 2006). Both TiO_2 and ZrO_2 single oxides exhibit excellent catalytic properties for various reactions, and both have been used as supports to disperse various noble and transition metals for distinct catalytic applications. The TiO_2 is unique for its photocatalytic and strong-metal-support-interaction (SMSI) properties, and the ZrO_2 is a well-known solid acid catalyst; both of them are n-type semiconductors. Most of studies report that by incorporating this element, one obtains superior photocatalytic performance. This is because the TiO_2-ZrO_2 mixed oxides exhibit high surface area, profound surface acid-base properties, high thermal stability, and strong mechanical strength. And, it is an established fact in the literature that active components dispersed on mixed metal oxides often produce superior catalysts to the one supported on single oxides for a number of reactions . It is known from modern catalytic surface science studies that the nature and quality of a carrier material is a key part of the catalyst. In addition to catalytic applications, these mixed oxides have

also been employed for various other purposes, such as photoconductive thin films, gas sensors, and in fuel cell and ceramic technologies (Reddy and Khan, 2005).

It is reported in the literature that mixing two dissimilar oxides adds another parameter since they are liable to form new stable compounds, which can lead to totally different physicochemical properties and catalytic behavior. Such advanced TiO_2-ZrO_2 mixed oxides not only take advantage of both TiO_2 (active catalyst and support) and ZrO_2 (acid-base properties), but also extend their application through the generation of new catalytic sites due to a strong interaction between them. In fact, the facile formation of zirconium titanate ($ZrTiO_4$) compound between ZrO_2 and TiO_2 exhibits excellent catalytic properties for various reactions (Reddy and Khan, 2005).

Hernández-Alonso *et al.* (2006) has optimized the characteristics of TiO_2-ZrO_2 thin films supported on borosilicate glass for the photocatalytic removal of VOCs by controlling the synthesis procedure. The photoactive oxides were deposited on ''Raschig rings'' of borosilicate glass using a dip-coating technique. The phase composition of the thin films was controlled during the sol preparation stage to produce either (1) $Ti_{0.90}Zr_{0.10}O_2$ solid solutions or (2) TiO_2/ZrO_2 binary metal oxides (10% and 20% molar content of Zr). For the structural parameters, the TiO_2/ZrO_2 samples showed that higher Zr content resulted in slight enlargement of the surface area, while the average pore diameter decreased. This may be because the presence of very small or/and amorphous particles of ZrO_2, which were not detected by XRD, hinderd the growth of anatase crystallites. And, the TG-DTA result revealed that the transition of anatase to rutile for undoped TiO_2 took place at 577°C while this structural transformation was not detected up to 750°C for samples containing Zr. So, these results confirm that the presence of Zr inhibits the transformation from anatase to rutile, leading to stabilizing the anatase phase. The samples having significant differences in the BET surface area present similar photoactivity, suggesting that the influence of the specific surface area on the efficiency of these processes seems to be modest. In any case, variations in the relative performance of the thin films with changes in pollutant and type of reactor suggest the importance of optimizing the characteristics of the photocatalytic coatings for each particular application.

Tian *et al.* (2009) prepared porous nanocrystalline S-doped TiO_2-ZrO_2 visible-light photocatalysts through a one-step method and evaluated the enhanced photocatalytic activity of the S-doped TiO_2-ZrO_2 in comparison to the S-doped TiO_2 and commercial Degussa P25. The photocatalytic activity of the S-doped TiO_2-ZrO_2 photocatalysts has been investigated in the visible-light region for the decomposition of Rhodamine B (RB) as a model pollutant. The results showed that the presence of ZrO_2 can increase specific surface area, even at the high calcination temperature, the surface area of S-doped TiO_2-ZrO_2 was still high if compared to S-doped TiO_2. These confirms that the introduction of ZrO_2 can significantly stabilize the porous structure and reinforce the thermal stability of S-doped TiO_2-ZrO_2. Moreover, ZrO_2 makes the catalyst possess more surface hydroxyl groups, which favors not only the trapping of electrons to enhance the separation efficiency of electron-hole pair but also the forming of surface free radical (•OH) to enhance the photocatalytic degradation of RB. For the photocatalytic activity, the maximum activity was obtained using the S-doped TiO_2-ZrO_2, which calcined at 500°C, because it had high surface area, small crystalline size, well-crystalline anatase phase, and intense absorption of the visible-light region, which are the results from introduction of ZrO_2.

2.9.1 Preparation of TiO_2-ZrO_2 Mixed Oxides

There are two types of combinations between TiO_2 and ZrO_2: physically mixed (with interaction forces being nothing more than weak Van der Waals forces) and chemically bonded (i.e. the formation of Ti–O–Zr linkages). When strong interaction is induced by chemical bonding, the physicochemical and reactivity properties of TiO_2-ZrO_2 mixed oxides will be very different from those of simple combinations of individual oxides (mechanical mixtures). The degree of interaction, or in other words, homogeneity or dispersion, largely depends on the preparation method and the synthesis conditions. Many different preparation methodologies have been employed to synthesize these mixed oxides.

The most widely employed methods to prepare TiO_2-ZrO_2 mixed oxides are coprecipitation and sol-gel. Other less frequently applied procedures include supercritical fluid (SCF) extraction (Weissman *et al.*, 1993), non-hydrolytic modified sol-gel (Andrianainarivelo *et al.*, 1997), and microwave-assisted combustion synthesis (Reddy *et al.*, 2007). An adequate synthetic methodology is a

fundamental starting point for developing any viable catalytic material. Among various preparation procedures available as mentioned above, coprecipitation has been most widely used, which is also termed wet precipitation in some reports. Sol-gel hydrolysis is also widely employed due to its capability in controlling the textural and surface properties of the resulting oxides. In sol-gel processes, domain formation due to the difference in the hydrolysis and condensation rates of Ti- and Zr-alkoxides has been identified as a major problem in the preparation of atomically dispersed mixed oxides. The preparation of zirconium titanate powder by a sol-gel route was reported by Navio *et al.* (1993), in which a hydroxoperoxo compound of Zr and Ti (HXPZT) was observed to be the reactive precursor, and this particular preparative strategy also received wide acceptability. Weissman *et al.* (1993) adopted a SCF extraction analogy to obtain TiO_2-ZrO_2 mixed oxide aerogels. In the SCF method, solvents were extracted from the gel without collapsing its structure, as would occur in conventional drying. The resulting aerogel had a high specific surface area.

Recently, a polymer gel templating technique was employed to make porous TiO_2-ZrO_2 mixed oxide networks. The photocatalytic efficiency of these oxides for photodecomposition of salicylic acid and 2-chlorophenol was found to be high. The wide-pore TiO_2-ZrO_2 mixed oxides were also synthesized by a low temperature sol-gel method followed by solvo-thermal treatment, and these materials were found to be highly promising for hydrotreating applications. Generally, the sol-gel synthesis by controlled hydrolysis of alkoxides or similar precursors are considered to be a suitable synthesis method, leading to a high degree of homogeneity. The underlying idea is that the preparation of gel or gel-like precursor should lead to a homogeneous dispersion at molecular level of Ti and Zr species, which upon calcinations, will lead to intimately formed mixed oxides (Reddy and Khan, 2005).

2.9.2 Structural Characteristics

In comparison to single oxides (surface area of TiO_2 = 20–200 m^2/g; surface area of ZrO_2 = 30–160 m^2/g), the mixed oxides (surface area of TiO_2-ZrO_2 = 85–430 m^2/g) exhibit higher surface area, stronger surface acidity, and higher thermal and mechanical strength. Since titanium and zirconium belong to the same group (IVB), they are expected to have similar physicochemical properties. When their oxides are formed together, the mutual interaction between them is expected to

be profound, which inhibits their individual crystallization. The observed significant changes in the specific surface area, acidity, basicity, and catalytic activity could be due to this strong mutual interaction. With the addition of zirconia to titania, the surface area of the mixed oxide increases sharply and reaches a maximum value for the mixed oxide having a Ti and Zr molar ratio of 1:1. The addition is also known to influence the crystallization pattern of both the oxides. In fact, they crystallize at higher temperatures when compared to that of single oxides (Reddy *et al.*, 1992).

The surface morphology and average surface roughness of TiO_2/ZrO_2 films were characterized by atomic force microscopy (AFM). The AFM images presented in Figure 2.15 revealed that the surface morphology of the mixed oxide film is very different from that of pure TiO_2 film. The crystallite size of the mixed oxide film is much smaller than that of pure TiO_2 film, indicating that the introduction of ZrO_2 suppresses the crystallite growth of TiO_2. As a result, nanometer films with smaller crystallite size are easily obtained. In addition, the average surface roughness of pure TiO_2 film is 1.487 nm, while that of mixed oxide film is 3.313 nm. The greater roughness is due to the discrepancy of the crystal lattices between $Zr_xTi_{1-x}O_2$ and TiO_2 (Reddy and Khan, 2005).

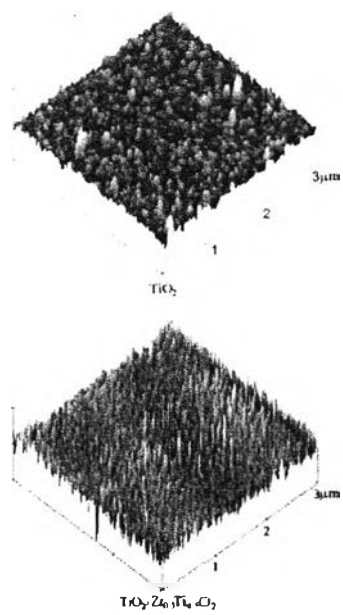

Figure 2.15 AFM images of pure and mixed TiO_2 films (Liu *et al.*, 2003)

2.9.3 Acid-Base Properties

The acid-base properties of oxide catalysts are very important for the development of scientific criteria in catalytic applications. The conversion and selectivity of a reaction not only depends on the nature of active sites, but also on their strength and number. Tanabe (1970) investigated the acid-base properties of several binary metal oxides. Their study sought to develop a theoretical basis for the generation of acidity in various binary oxides, which is non-existent in the constituent single oxides. A fairly good correlation was demonstrated between the observed highest acid strengths and the average electronegativities of metal ions of the binary oxides. Tanabe's model can be applied to dilute mixed oxides where a small amount of a second oxide is incorporated into the first oxide by cation substitution. This model assumes that the generation of new acid sites is caused by an excess of negative or positive charge in a model structure of the binary oxide. The model structure constructed is as follows: (i) the coordination number of a cation of the component oxide is maintained in the binary oxide, and (ii) the coordination number of the oxygen ion in the binary oxide is the same as in the major component oxide. This model has been applied to many binary oxides, including TiO_2-ZrO_2. The TiO_2-ZrO_2 binary oxide has shown affirmative results. The high success rate makes this model highly useful, although it is limited by the assumptions used. One limitation is the need to have a unique coordination number, which may be difficult to decide in systems of low symmetry. Another limitation is the use of formal oxidation states, which may be quite different from the real charge. Since electron deficiency at a site refers to real charge at the site, the use of formal oxidation states may not be accurate. Finally, the model cannot predict acid strength. However, there appears to be a rough correlation between electronegativity of the cations and the strength of acid sites in many mixed oxides.

The interaction between the two oxides results in a significantly greater surface acidity than that of the single component oxides. The maximum value of acidity occur at about 50 wt.% TiO_2 (TiO_2/ZrO_2 = 1/1). These findings are consistent with the Tanabe's model, where new acid sites are associated with Ti-O-Zr linkages. It is also quite possible that as the transition metal oxide particle size decreases, the number of surface oxygen anion vacancies increases, hence new and stronger acid

sites are created, with the particles of smallest diameter having the strongest acidity. The TiO_2-ZrO_2 mixed oxides can be thought as a mixture of relatively small particles contributing acidity from anion vacancies, in addition to the surface acidity arising from interactions postulated by Tanabe (1970). The acid-base characteristics of TiO_2-ZrO_2 mixed oxides and the corresponding variously promoted samples were extensively investigated using different test reactions, such as TPD, in-situ FTIR, and other techniques (Reddy and Khan, 2005).

2.10. Porous Material

The classification of pores according to size has been under discussion for many years, but in the past, the terms ''micropore'' and ''macropore'' have been applied in different ways by physical chemists and some other scientists. With an attempt to clarify this situation, the limits of size of the different categories of pores included in Table 2.1 have been proposed by the International Union of Pure and Applied Chemistry (IUPAC) (Ishizaki *et al.*, 1988 and Rouquerol *et al.*, 1999). As indicated, the ''pore size'' is generally specified as the ''pore width'', i.e. the available distance between the two opposite walls. Obviously, pore size has a precise meaning when the geometrical shape is well defined. Nevertheless, for most purposes, the limiting size is that of the smallest dimension, and this is generally taken to represent the effective pore size.

Table 2.1 Definitions about porous solids

Term	Definition*
Porous solid	Solid with cavities or channels which are deeper than they are wide
Micropore	Pore of internal width less than 2 nm
Mesopore	Pore of internal width between 2 and 50 nm
Macropore	Pore of internal width greater than 50 nm
Pore size	Pore width (diameter of cylindrical pore or distance between opposite walls of slit)
Pore volume	Volume of pores determined by stated method
Surface area	Extent of total surface area determined by given method under stated conditions

According to the IUPAC classification, porous materials are regularly organized into three categories on a basis of predominant pore size as follows:

- Microporous materials (pore size < 2 nm) include amorphous silica and inorganic gel to crystalline materials, such as zeolites, aluminophosphates, gallophosphates, and related materials.

- Mesoporous materials (2 nm ≤ pore size ≤ 50 nm) include the M41S family (e.g. MCM-41, MCM-48, MCM-50, and etc.) and other non-silica materials synthesized via intercalation of layered materials, such as double hydroxides, metal (titanium, zirconium) phosphates, and clays.

- Macroporous materials (pore size > 50 nm) include glass-related materials, aerogels, and xerogels.

Nowadays, micro- and mesoporous materials are generally called ''nanoporous materials''. Particularly, mesoporous materials are remarkably very suitable for catalysis applications, whereas the pores of microporous materials may become easily plugged during catalyst preparation if high loading is required.